Experimental characterization of H-VAWT turbine for development of a digital twin

Leblanc, Bruce; Ferreira, Carlos

DOI
10.1088/1742-6596/1452/1/012057

Publication date
2020

Document Version
Final published version

Published in
Journal of Physics: Conference Series

Experimental characterization of H-VAWT turbine for development of a digital twin

Experimental characterization of H-VAWT turbine for development of a digital twin

Bruce LeBlanc and Carlos Ferreira
Delft University of Technology, Kluyverweg 1, Delft, The Netherlands 2629HS
E-mail: b.p.leblanc@tudelft.nl

Abstract. A digital twin can be described as a digital replica of a physical asset. The use of such models is key to understanding complex loading phenomena experienced during testing of vertical axis wind turbines. Unsteady aerodynamic and structural effects such as dynamic stall and dynamically changing thrust and blade loading are difficult to predict with certainty. This leads to inefficient turbine designs or worse yet premature failures. Many of these phenomena can be better understood through scaled wind tunnel testing. The analysis of these test results is greatly improved by having a well calibrated digital twin model of the turbine. This paper discusses the methodologies used in the development of the model for a H style vertical axis wind turbine. This includes physical measurements of the as built system, updates to the models based upon experimental testing and a final correlation between test and model on a component by component as well as fully assembled system.

Nomenclature

CAD Computer-aided Design
DOF Degree of Freedom
EMA Experimental Modal Analysis
FEA Finite Element Analysis
FRF Frequency Response Function
$IEPE$ Integrated Electronics Piezo-Electric
$LCOE$ Levelized Cost of Energy
MAC Modal Assurance Criterion
MPE Modal Parameter Estimation
OJF Open Jet Facility
$SIMO$ Single Input Multiple Output
TSR Tip Speed Ratio
$VAWT$ Vertical Axis Wind Turbine

1. Introduction

One of the potential solutions for reducing the Levelized Cost of Energy (LCOE) of floating offshore wind turbines is by transitioning to a vertical axis orientation. Due to a lower center of gravity and higher maximum tilt threshold than conventional horizontal axis orientations it may

be possible to drastically reduce the amount of steel required for the support structure. One of the findings of recent works studying these effects [1, 2, 3] is that in order to reduce thrust loading in high wind and wave conditions, individual pitch control may be required. Due to pitching requirements, a lot of recent efforts have been focused on the "H" configuration with generally straight blade geometries. Due to the cross-flow design of the Vertical Axis Wind Turbine (VAWT) thrust and blade loading vary substantially with azimuth position during rotation. Depending on Tip Speed Ratio (TSR), the azimuthally varying angle of attack on the blades can lead to large amounts of dynamic stall every rotation. It is of interest to study the loading dynamics of these phenomena in order to improve the design of VAWTs and to better inform floating platform design. To that end, a $1.5mx1.5m$ H-VAWT, referred to as PitchVAWT, with active pitch capability has been designed and operated at Delft University of Technology [4, 5]. This model is used to validate turbine performance codes and to study the loading behaviors of actively pitched VAWTs in different TSRs and pitching configurations. A finite element model of the turbine was made to understand the effect of changes in aerodynamic loading on the thrust and blade reaction loads. It is also used as a check to properly design future tests in order to operate the turbine in stable conditions. To be confident what is predicted by the models correctly matches the test data, it is important to make sure the model is as representative of reality as much as possible.

It has been shown that modal test data is a good way of estimating the uncertain material parameters used in modelling [6] and has been used for many years on wind energy systems[7, 8, 9, 10, 11, 12]. Modal testing provides a way of validating the models such that the overall mass, stiffness, and boundary conditions of the system can be accurately captured. Whereas traditional static testing such as 3 point bend tests and overall weight measurements will not properly provide all necessary detail.

Therefore a series of tests were performed on the PitchVAWT turbine in order to ensure the digital twin finite element models correctly match reality. Each major component of the turbine, the blades, the struts, the mounting platform and the fully assembled system are checked for consistency with the corresponding digital model.

2. Turbine Description

The PitchVAWT turbine is a two-bladed H-shaped vertical axis wind turbine with two horizontal struts on each blade mounted at approximately 24% and 76% of the blade height. The turbine rotor has both a height and diameter of $1.5m$. Overall turbine design specifications are given in Table 1. The NACA0021 airfoil was chosen for blade geometry due to its fairly common use in VAWT research and its relative thickness for structural stability. The chord-radius ratio of 0.1 was chosen to minimize the effects of flow curvature. A set of thrust bearings transfer the thrust and weight of the rotor to the structural base of the turbine while allowing the rotation and torque to be passed through a torque and speed sensor. The drive-line then extends from the torque sensor to the generator / motor at the very base of the turbine. The full turbine system is then mounted to a blue positioning lift which acts as a foundation for the turbine system. A picture of the installed turbine at the Open Jet Facility in Delft, The Netherlands is shown in Figure 1, with a dimensioned drawing given in Figure 2.

As for turbine component materials, the rotor blades and struts are manufactured from extruded aluminum. The set of struts and blade sets were manufactured by different independent producers, therefore the material properties will be quantified separately. The tower is made of steel tubing with a 60 mm outer diameter and wall thickness of 5 mm. The main bearing housing consists of a 115 mm diameter steel tube, with 5 mm wall thickness which secures the two thrust bearings. The turbine base is made of standard 50 mm square tubing welded together in the shown box shape with two mounting platforms made of 20 mm thick aluminum plates. The top plate acts as a base of the rotor, and the bottom plate holds the turbine drive unit.

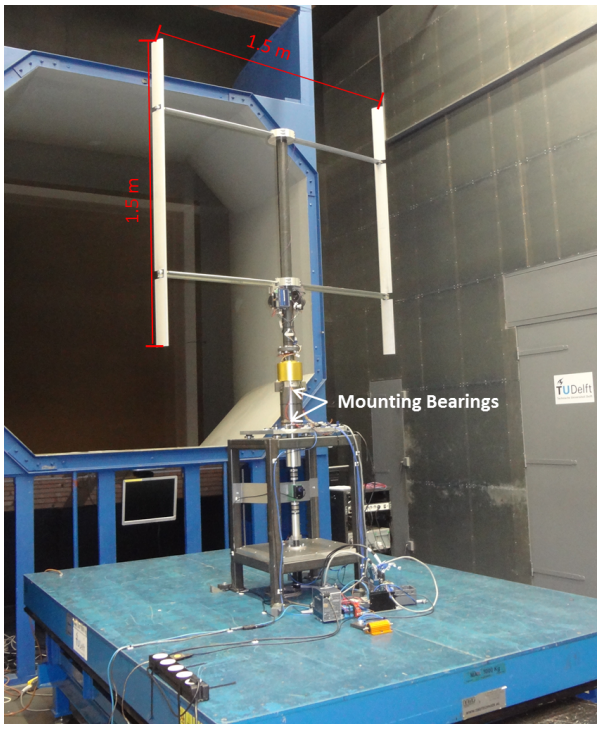

Figure 1. PitchVAWT installed in Open Jet Facility

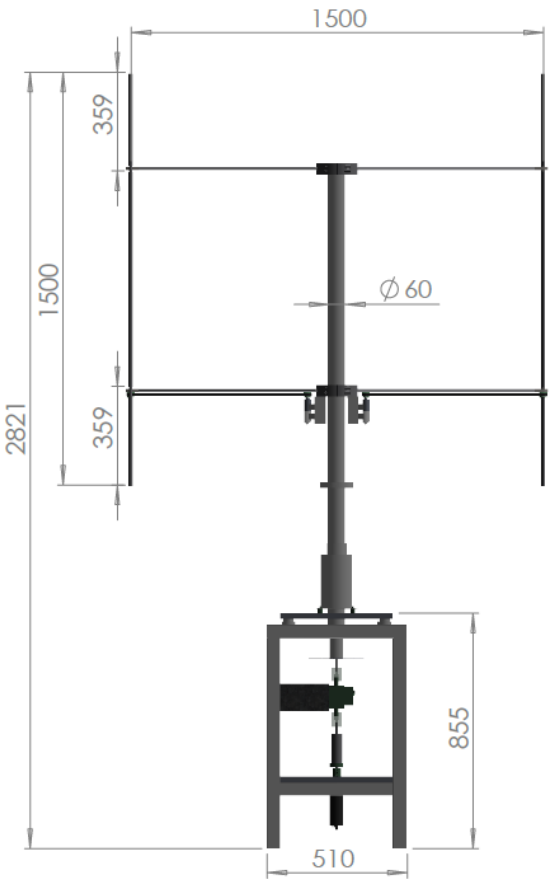

Figure 2. PitchVAWT CAD model, dimensions in *mm*

Table 1. PitchVAWT Design Specifications

Property	Dimension
NBlades	2
NStruts	4
Height	1.5 m
Diameter	1.5 m
Blade Chord	0.075 m
Strut Chord	0.060 m
Solidity	0.1
Blade Airfoil	NACA0021
Strut Airfoil	NACA0018
Operating TSR	1 - 4

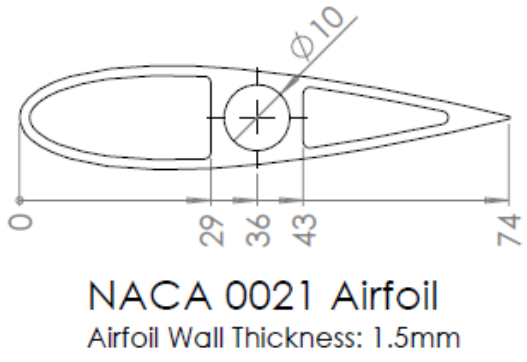

Figure 3. Blade cross-section

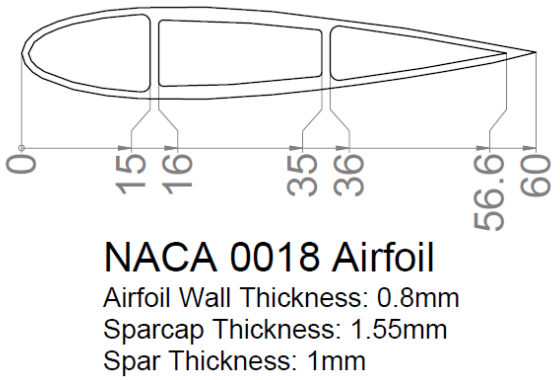

Figure 4. Strut cross-section

3. Testing Methods

Individual tests are performed to measure:

- As-built dimensions of components and full turbine
- material properties of blades and struts
- Frequencies and mode shapes of turbine and components
- representative grounding spring stiffness values for flexible blue platform

The approach is to verify as many physical properties as possible through independent measurements. For example, in going from the design concept of the blade to a calibrated finite element model there are several unknowns which need to be verified: the actual material density and elastic modulus, the as produced geometry, and the boundary conditions which support the said blade on the turbine. The length of the blades are verified using a tape measure. The profile of the blade is measured with a Coordinate Measurement Machine and used to calculate the cross sectional area and moment of inertia about each axis. The weight of the blades is then measured with a Kern 16K0.1 platform scale reproducible to the nearest 0.1 gram. Knowing the length, cross sectional area, and weight of the blades allowed the calculation of the material density. The two properties left to verify are the material stiffness and the boundary conditions of the blade on the turbine. A free-free modal test removes the effect of boundary condition, thereby allowing the stiffness of the material to be altered to match the natural frequencies of the blade. With a calibrated free-free model, the full turbine modal test is used to identify the boundary conditions of the attachments. This procedure was also performed for the struts.

The platform dimensions were measured with standard tape measures and was tested with EMA prior to turbine installation in the height configuration used for the testing. Standard material models for steel were used as initial guesses. The 6 rigid body modes are used to tune the support springs, and the flexible modes are used to tune the material stiffness of the beam elements. These tests are used to update the finite element model properties of each component independently. The full turbine is then tested while mounted to the platform in the open jet facility wind tunnel to verify the boundary conditions of the connections between each component.

Experimental Modal Analysis with impact testing was performed for each structure in a Single Input Multiple Output (SIMO) format. EMA consists of measuring a series of excitation and response between degrees of freedom of the structure. Traditionally a force transducer is used to measure the force excitation imparted into the structure at a given degree of freedom, DOF, and an accelerometer is used to measure the response of the structure. A transfer function is

calculated between the excited and the measured DOF, this is known as the Frequency Response Function or FRF. A transfer function is required between each DOF in order to understand the global motion of the structure due to a given input. The collection of FRFs relating each output DOF and response DOF is referred to as the FRF matrix. Each FRF is then curve fit with a specific polynomial which has been designed to extract dynamic characteristics of the response including magnitude and phase of the DOF motion as well as the natural frequency and damping characteristics of each mode, this is referred to as Modal Parameter Estimation or MPE. This test takes advantage of the concept of reciprocity, which means that the transfer function between the force and response degrees of freedom is independent of direction. Which in practice means that it is not necessary to measure both response and force at each DOF. A response measurement is required so that each mode can be visualized independent of other modes, but is not necessary at every DOF. The force measurement is "roved" between all test DOF. In this manner, the full FRF matrix can be assembled.

The blade and strut, referred to for simplicity as "beam", component tests used a single accelerometer located at the end of the beam and the hammer was roved to each measurement point. This was completed for both flapwise and edgewise modes. Measurements were taken with the beam hung horizontally from an overhead support using two long strings. The strings were aligned with the expected location of the nodes for the first bending mode so as to minimize the effects of the supports on the measured modes. The beam is rotated in the supports so that the axis which is being measured is normal to the support. Thus providing minimal support effects in the measured direction. The blade was measured with 22 measurement locations evenly distributed across the blades, while the struts were measured with 5 evenly distributed locations. Figures 5 and 6 show the test setup and accelerometer mounting for the blade / strut free-free modal tests.

After initial modeling of the platform showed several modes of interest in the frequency range of interest, it was decided to perform a more detailed modal survey of the platform. The testing geometry composed 52 measurement locations in X, Y, and Z directions across the turbine with ten averages at each point. For certain locations it is not possible to physically impact the point in each dimension (like impacting inside the plane of the platform), for these locations slave degrees of freedom to proper adjacent points were used in order to correctly visualize the mode shapes. Three tear-drop IEPE based accelerometers were placed in the X, Y, and Z directions of point 1 located on the top corner of the plate. This corresponds to 73 impact locations and 3 response measurements with 10 impacts per location. Figures 7 and 8 show the test setup and accelerometers mounted for the platform modal test.

The test geometry of the full turbine is shown in figure 9. Impacts are made at 42 locations in X, Y, and Z directions distributed across the turbine system with five averages at each

Figure 5. Accelerometer blade flapwise test

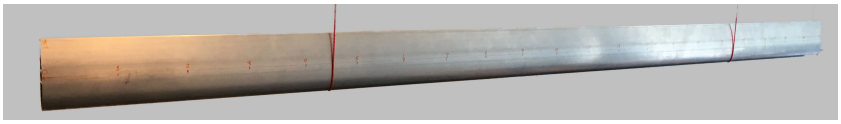

Figure 6. Blade Free-Free boundary condition setup

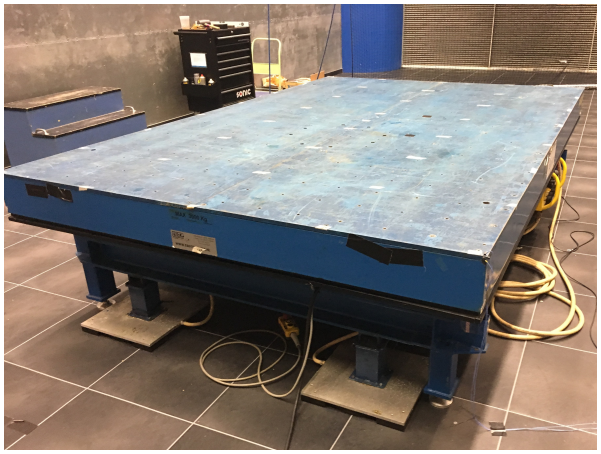

Figure 7. Platform modal setup

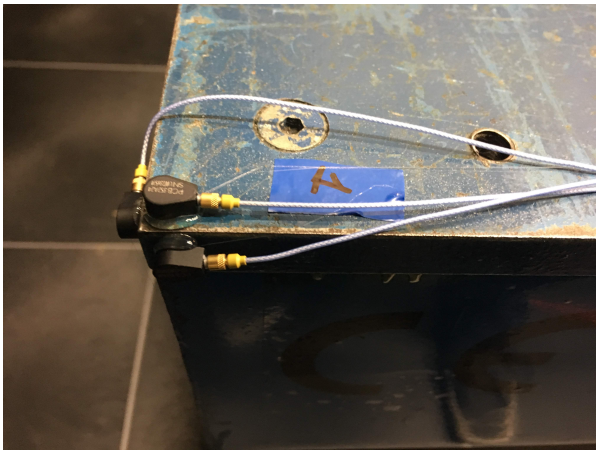

Figure 8. Accelerometers on platform

measurement location. The response of the turbine is measured by a set of six tear drop accelerometers placed in the X, Y, and Z directions of the corner of the platform, and the X, Y, and Z directions on the bottom of the first blade. The locations are chosen in order to properly capture modal dynamics in the three translational directions within the frequency range of interest. In total 6 reference measurements are made from 100 impact locations with 5 averages for each location.

3.1. Data Collection and Processing

Data was collected using National Instruments^{TM}CDAQ hardware and LabView at a sampling rate of 2560 samples / second. Each data block lasts 10 seconds. No windows have been used in the collection of the data. The averaged autopowers for the platform drive-point impact measurement during the full turbine testing are shown with the X, Y, Z response in Figure 10. This shows the frequency range excitation of the impact is relatively flat throughout the range of interest, meaning the modes should be properly excited.

The three reference accelerometers on the platform were shown to be sufficient to properly capture the dynamics of the full system in the lower frequency range up to 40 Hz. The sum of all FRFs for all three directions from the platform reference accelerometers is shown in figure 11. This measurement gives insight into just how many modes the full structure has between 5 and 18 Hz. Data post-processing and Modal Parameter Estimation, MPE is performed within Siemens^{TM}Test.lab software using the Polymax curve-fitter. After calculation of the mode shapes individual FRFs are then synthesized based on the fit modes. The synthesized FRFs should compare well with each measured FRF if the modes have been properly characterized. An example of one of these comparisons is given in Figure 12. Modes have been fit in this case up to a frequency of 40 Hz. Each vertical line represents the frequency where a mode was found. The magnitude and phase of the synthesized FRF matches the measurement closely throughout the range of interest. This process is performed on all EMA tests of the individual components as well as the full turbine system.

3.2. Model Correlation

The model is compared with test data on two major criteria, the natural frequency of the modes and the similarity of the mode shape vectors themselves. The correlation between mode shape vectors will be made using the Modal Assurance Criterion, MAC[13, 14], shown in equation 1. MAC is a correlation tool which compares each modal vector. A MAC value of 1 corresponds

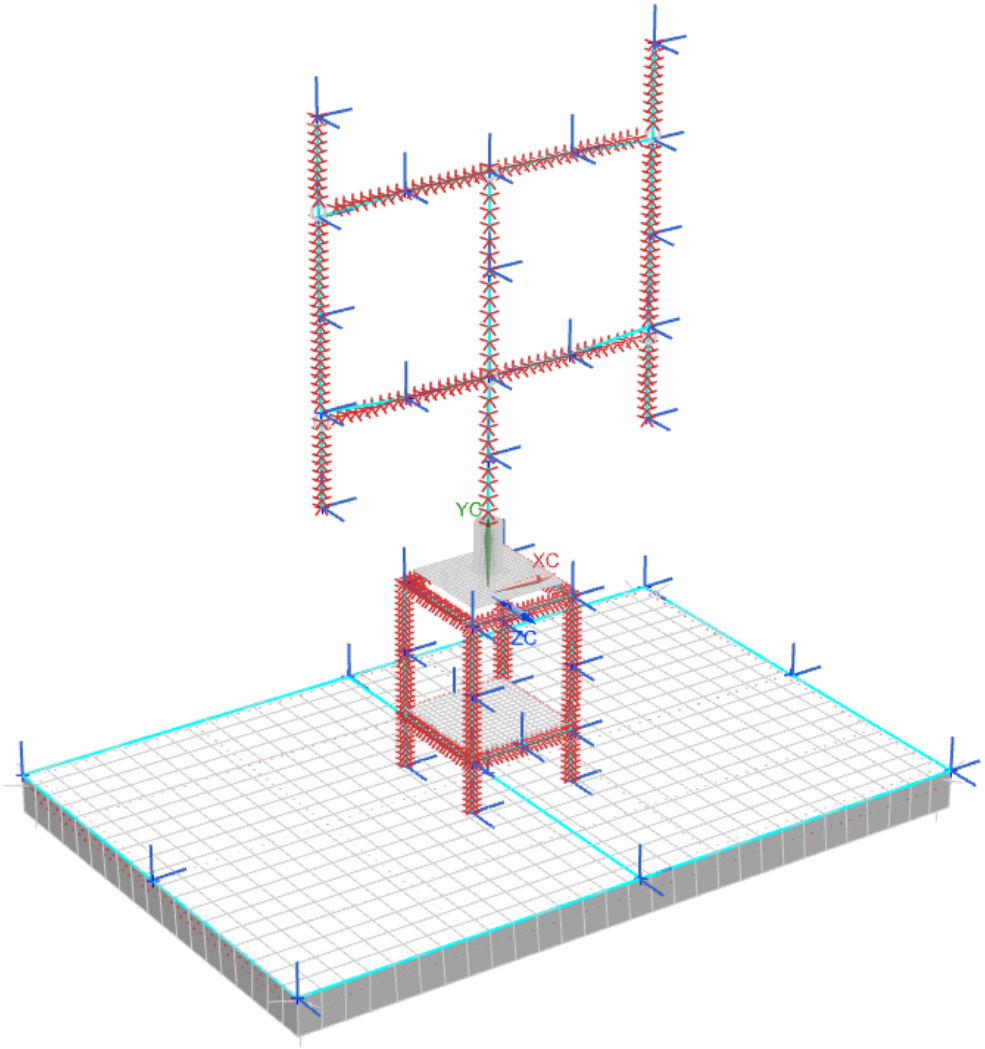

Figure 9. Experimental test geometry with impact directions shown as long blue arrows overlaid on the finite element model including all 42 test impact locations

to a perfectly correlated mode shape pair, meaning mode shape vectors are exactly the same, while a MAC value of 0 implies no correlation between the shapes. While not a comprehensive measure, it provides good insight into the behaviour of the model with respect to the test data.

$$MAC = \frac{[[U]^T[E]]^2}{[[U]^T[U]][[E]^T[E]]} \tag{1}$$

Where:
U = Mode shape vectors of FEA
E = Mode shape vectors from EMA
T = Transpose

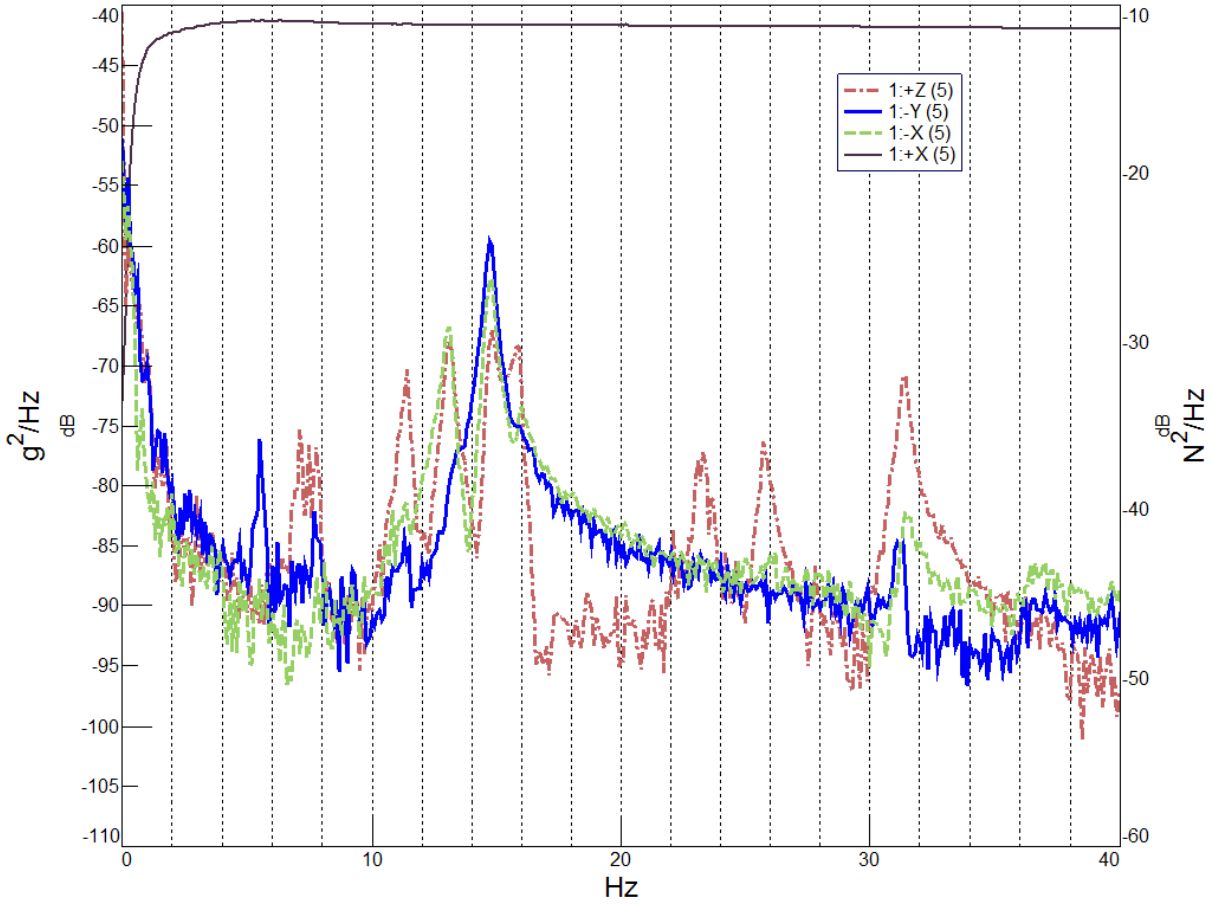

Figure 10. Averaged autopowers of impact and response at drive-point on platform

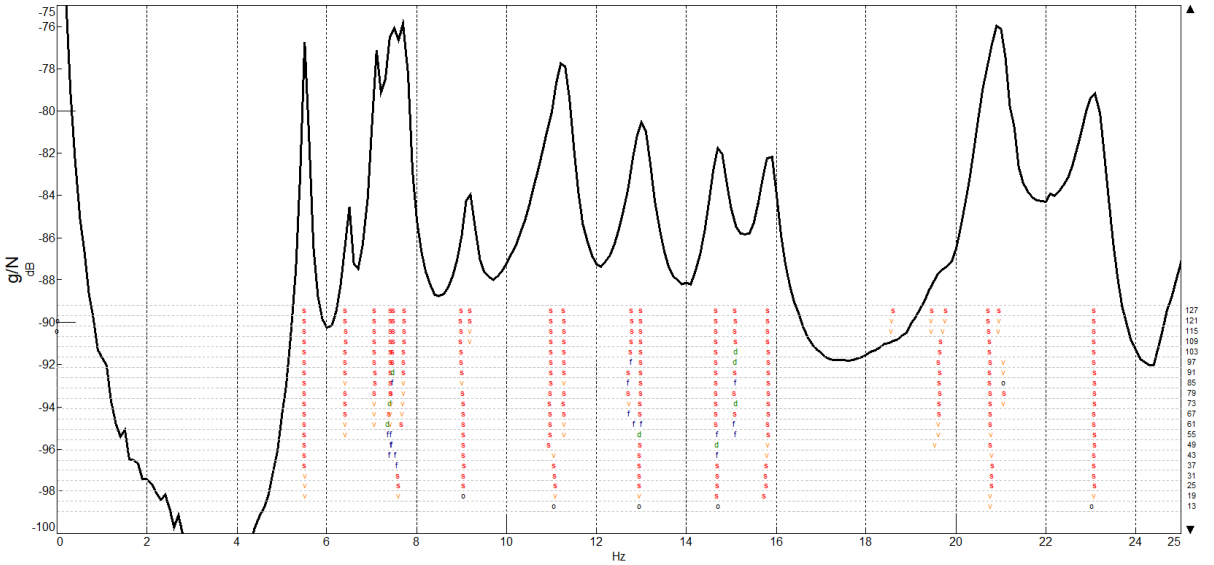

Figure 11. Sum of included FRFs on the full turbine system from platform mounted accelerometers with overlaid stabilization diagram, each "s" represents a stable pole

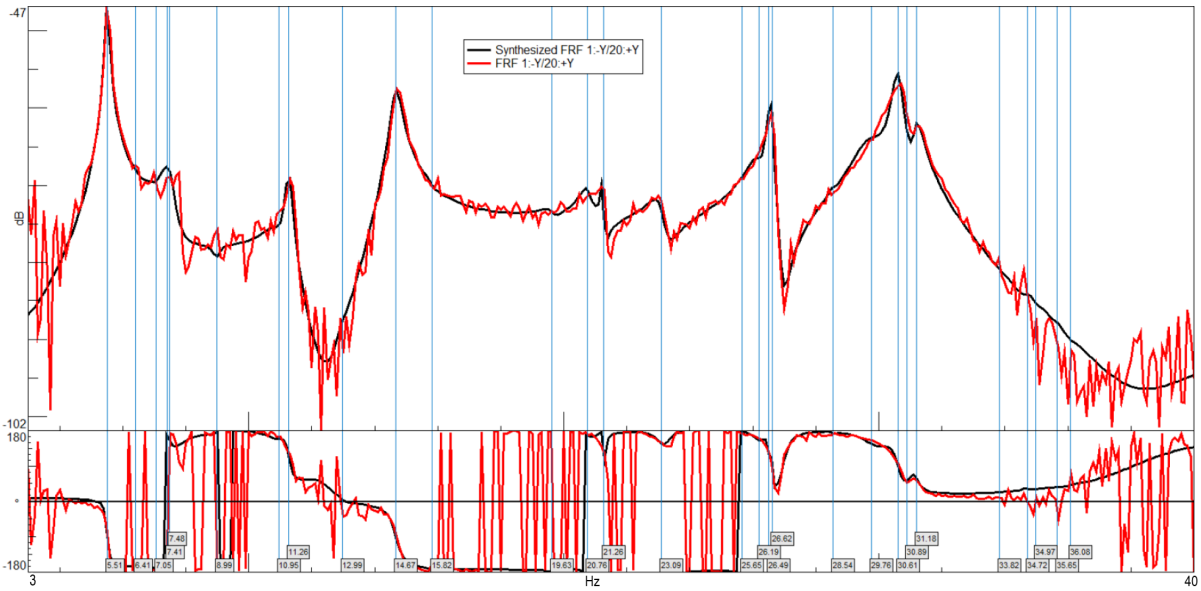

Figure 12. Example of a synthesized FRF (black) with a measured FRF (red) from the fit mode shapes(blue vertical lines).

4. Testing Results

The blades, struts, and platform have been each measured using a variety of techniques in order to verify the assumptions of the finite element models. The full system was then tested in-situ at the Open Jet Facility wind tunnel in Delft. The results of these tests are given here.

4.1. Blades and struts

A set of measurements have been carried out in order to determine the actual length and mass of the blades. Three blades were measured to understand the variability of the manufacturing process for the blades. These measurements together with the previously measured cross sectional properties of the blade, allowed the density of the material to be calculated. Results of the three individually tested blades are shown in table 2. The average values of the three blades were used to update the blade length to 1.508 meters and density to 2707 kg/m^3 in the model. The density of the strut material was measured directly to be 2620 kg/m^3 by measuring a small sample of the material with a DeltaRange AG204 analytical balance.

The first five flexible modes of two independent blades were extracted from measurement data. The natural frequency and damping values for each mode are shown in Table 3. The values for each blade are very similar, with the largest % difference in frequency being 0.18%. The conclusion from this is that the two blades are very consistent from the manufacturing process with minimal variation between each blade.

Table 2. Measurements of Blade Properties

Blade Number	**length**(m)	**Section Area** (mm^2)	**Weight**(kg)	**Density**$(\frac{kg}{m^3})$
Blade 1	1.508	303	1.2332	2699
Blade 2	1.508	303	1.2400	2713
Blade 3	1.508	303	1.2380	2709
Average	1.508	303	1.2371	2707

Table 3. Variability in Modes Between Blades

Mode	**B1 F(Hz)**	**B1 Damp(%)**	**B2 F(Hz)**	**B2 Damp(%)**	**% Diff Freq**
1	38.10	0.11	38.12	0.38	.06
2	104.79	0.14	104.98	0.14	0.18
3	204.80	0.06	204.99	0.06	0.09
4	336.83	0.07	337.20	0.08	0.11
5	499.95	0.05	500.60	0.04	0.13

The first four flexible modes for the blades and struts are given in Table 4. As to be expected based upon the geometry of the airfoils, the flapwise modes are substantially lower in frequency than the edgewise and the structural damping values are all very low due to being Aluminum extrusions. The frequency ranges for the free-free blades are very high with respect to the turbine operating frequencies (up to 3 Hz). This is a by-product of being designed for minimal displacement during rotation at high speeds for use with laser and photographic imaging systems like Particle Image Velocimetry.

4.2. Platform Structure

The platform where the turbine is mounted in the tunnel plays a critical role in the overall system dynamics. It is made of a $2mx3mx0.015m$ steel sheet supported by a scissor lift frame. The rigid body modes of the "floating" support structure can be close to the 2P excitation frequency of the turbine during operation and needs to be studied in detail. The first flexible modes of the full platform begin to occur in the 20 Hz range. The mode shapes for the first rigid body mode and first flexible mode are given in Figures 13 and 14 respectfully. The natural frequencies and damping values for the modes of interest are given in Table 5.

4.3. Full Turbine

The natural frequency and damping values for each mode are shown in table 6. As some of the mode shapes are non-standard, the description of them can be difficult to relate, however, an attempt has been made. Sixteen modes were fit in this frequency range showing a varied set of both rigid body and flexible motion from the platform as well as several flexible rotor modes. These modes were then used to re-synthesize the FRFs. These give a measure of how well the modes were fit. An example of the synthesized FRFs are shown in Figure 12. The

Table 4. Natural Frequency and Damping Values of Flexible Modes for Blades and Struts

Mode	**Description**	**Frequency(Hz)**	**Damping(%)**
	Blade		
1	first flap-wise	38.10	0.11
2	second flap-wise	104.79	0.14
3	first edge-wise	144.25	0.09
4	third flap-wise	204.80	0.06
	Strut		
1	first flap-wise	116.19	.04
2	second flap-wise	317.87	.05
3	first edge-wise	471.28	.03
4	second edge-wise	1257.22	.04

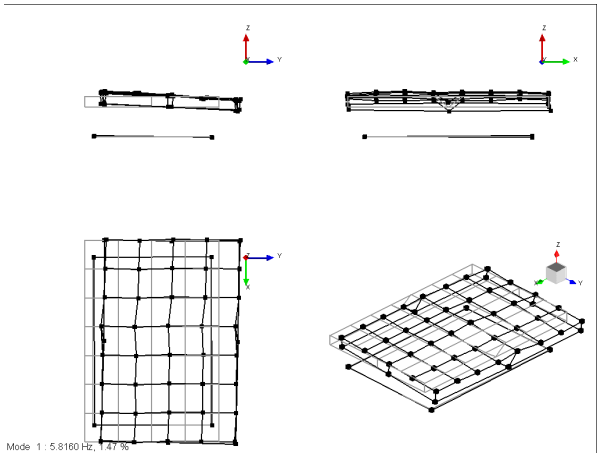

Figure 13. First side-side Rigid Body Mode of platform at $5.8Hz$

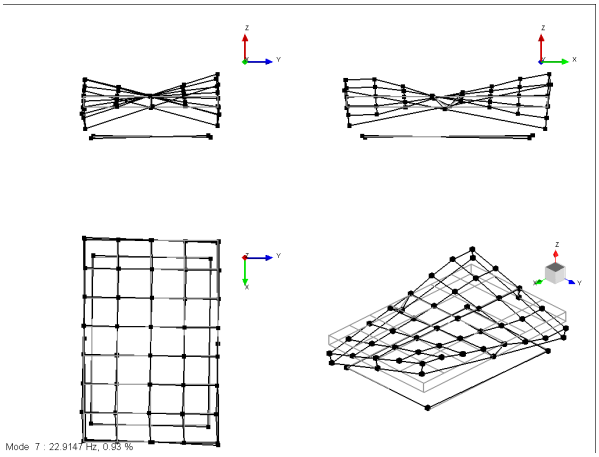

Figure 14. First torsion flexible mode of platform at $22.9Hz$

Table 5. Natural Frequency and Damping Values of Platform Structure

Mode	Description	F(Hz)	Damping(%)
1	side-side rigid	5.81	1.47
2	vertical bounce rigid	7.28	1.6
3	rotation about x-axis rigid	9.78	2.06
4	fore-aft rigid with rocking	12.71	2.4
5	rotation about z-axis rigid	15.68	2.27
6	rotation about y-axis rigid	16.294	1.68
7	first torsion	22.915	0.93
8	first bending with drum	28.84	1.46

synthesized FRFs fit the data well for the given responses, and is mostly consistent throughout the measurement range. At higher frequencies the sparsity of the test geometry prevents properly tracking modes with large amounts of curvature. An example of the first platform side to side rigid body mode is shown in Figure 15

5. Correlation and Updating

As stated above, the goal of the updating process is to independently verify the assumptions used in the modelling of the turbine with various measurement techniques on the as built system. These changes are propagated to the models of each component and compared with reality using the correlation of mode shapes and the values of the predicted natural frequencies.

5.1. Blades and Struts

The measurements of the lengths, cross sectional areas, and densities of the blades and struts are directly applied to the representative beam models. The material stiffness of the blades and struts are then tuned to match the measured natural frequencies. The updated material properties for the blades and struts are given in Table 7. The blades and struts are relatively simple to model and the results of the free-free modal tests compare very closely with the expected natural frequencies and MAC values for each mode. The correlation results are shown in Table 8. The first four flapwise bending modes of the blades show shown in Figure 16. The finite element model overlays well with measured mode shapes for each mode.

Table 6. List of Modes of Full Turbine Installed in OJF

Mode	Description	Frequency (Hz)	Damping (%)
1	table side-side	5.506	0.97
2	strut vertical blades out of phase	6.406	1
3	strut vertical blades in phase table in phase	7.061	0.71
4	strut vertical blades in phase table out phase	7.412	0.9
5	platform rock in phase with tower side side	7.48	3.16
6	platform rock out of phase with tower side side	7.712	0.63
7	tower fore-aft	9.051	1.19
8	tower side-side table rock out of phase	10.996	3.42
9	platform rock side-side turbine flexible at bearing	11.288	1.03
10	platform rock fore-aft flexible struts	12.961	1.12
11	platform twist	14.676	1.08
12	platform rock fore-aft	15.824	1.02
13	rotor strut rock out of phase	19.649	0.75
14	rotor strut rock in phase	20.767	0.97
15	platform torsion	23.088	1.17
16	platform vertical drum mode	25.653	1.1

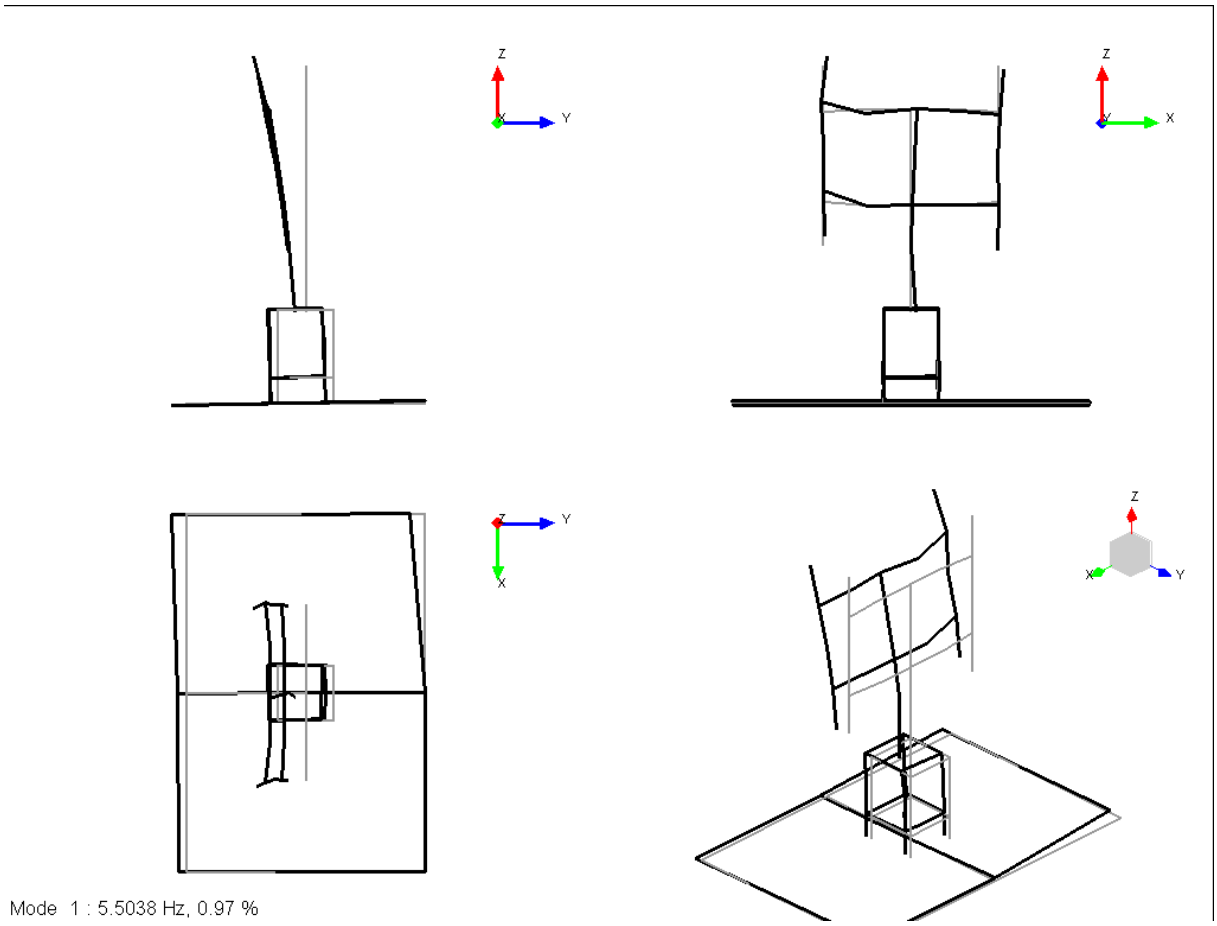

Figure 15. First mode of platform rocking at 5.5 Hz

Table 7. Updated Material Properties for Blades and Struts

Property	**Dimension**
ρ_{Blade}	$2707\,\mathrm{kg/m^3}$
ρ_{Strut}	$2620\,\mathrm{kg/m^3}$
E_{Blade}	69 GPa
E_{Strut}	55 GPa

Table 8. Blade and strut free-free EMA vs FEA updated properties

Mode	**EMA Freq(Hz)**	**FEA Freq(Hz)**	**% Diff**	**MAC**
Blade				
1	38.10	37.97	-0.33	0.996
2	104.79	104.66	-0.12	0.997
3	204.80	205.19	0.18	0.997
4	336.83	339.21	0.71	0.995
Strut				
1	116.19	117.75	1.34	0.999
2	317.87	323.05	1.62	0.995
3	471.28	424.19	-9.99	0.995
4	616.04	628.22	1.98	0.998

5.2. Platform

As discussed above, the platform consists of a frame structure composed of square tubular steel with a steel plate bolted on top. An under view of the fem model is shown in Figure 17 giving a view of the frame construction. The scissor-lift structure is approximated by attaching grounding springs in the X, Y, and Z translational directions at each location where the scissor lift mates to the frame. Figure 18 shows the layout of the spring attachments from a top down view. The platform dimensions were measured with standard tape measures and input directly into the model. It was not possible to measure the mass of the entire platform due to its size so standard material models for steel were used. The important take away for the model of the table is a representative boundary condition for the turbine, so as long as the equivalent dynamics of the frame and support match the measured data, the model is considered accurate enough for this purpose. The rigid body modes of the platform are used to tune the support springs. The tuning of the springs was achieved through a multi-objective genetic algorithm optimization of each spring stiffness with the target being to maximize the MAC value and minimizing the difference in frequency between each mode pair. The results of the optimization for each spring stiffness is given in Table 9.

The correlation of the rigid body modes and first two flexible modes for the platform are given in Table 10. The rigid body mode frequencies and mode shapes align fairly well which points to the tuning of the mounting spring constants and the general accuracy of the layout of the frame structure. However, not all modes are matched perfectly, such as the twisting of the platform, and this can be seen as a limitation of replacing the actual scissor lift structure with this set of simple springs. For the purposes of being a boundary condition to the overall turbine performance, the results are considered valid.

5.3. Full Turbine Assembly

For the fully assembled turbine, the independently calibrated finite element models of the platform, blades, and struts are mated together along with models of the turbine base and tower

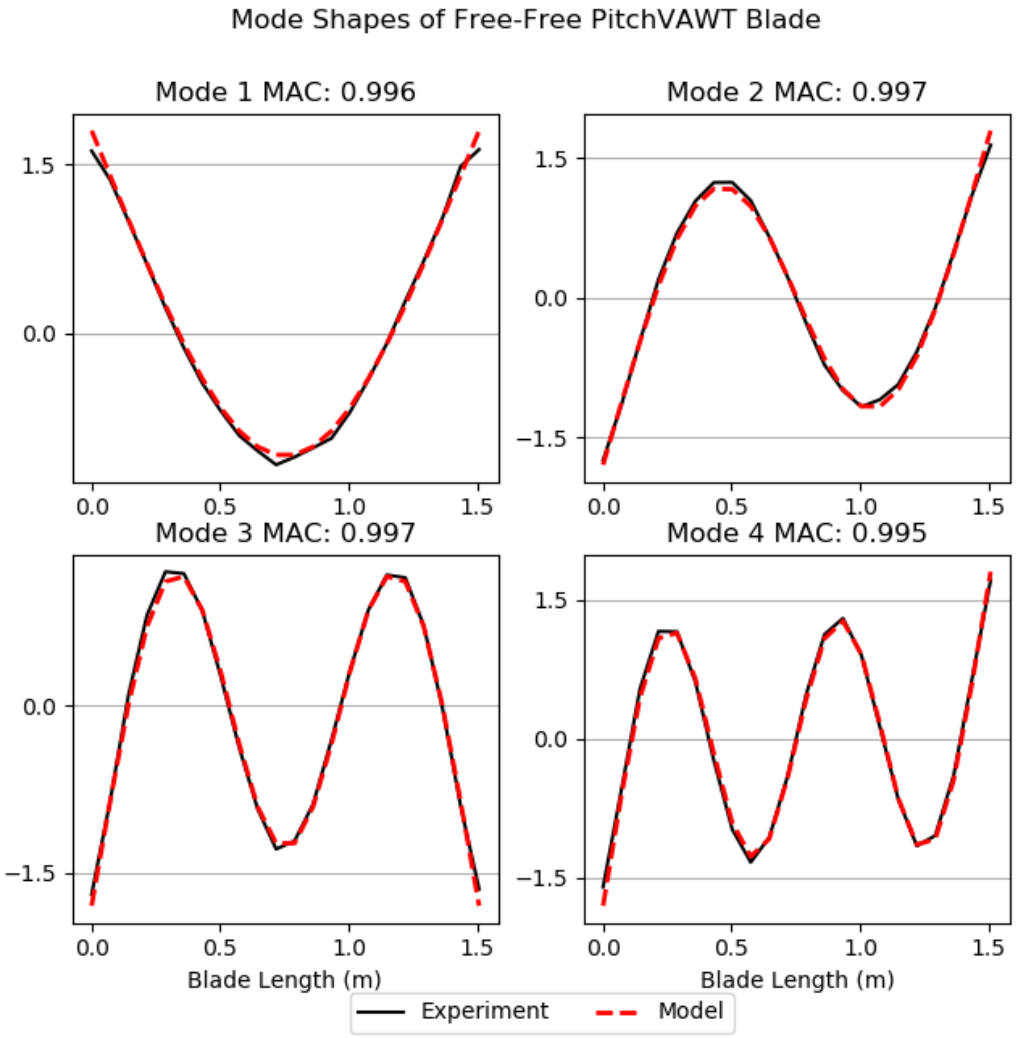

Figure 16. Overlay of first 4 flexible modes of turbine blade, Unit Modal Mass scaling

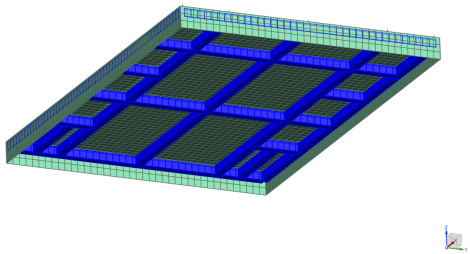

Figure 17. Finite element model of platform

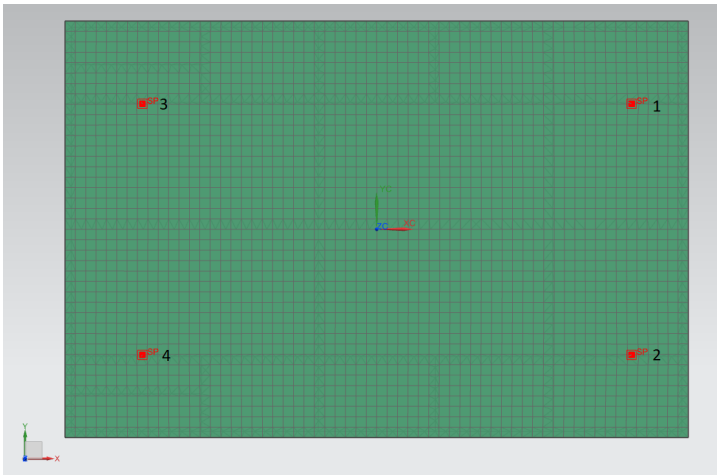

Figure 18. Layout of spring connections for platform

Table 9. Updated Platform Grounding Spring Stiffness

Property	Dimension
$Spring1_X$	20 387.6 N/mm
$Spring1_Y$	567.2 N/mm
$Spring1_Z$	2343.7 N/mm
$Spring2_X$	8637.6 N/mm
$Spring2_Y$	601.6 N/mm
$Spring2_Z$	1888.5 N/mm
$Spring3_X$	8254.5 N/mm
$Spring3_Y$	329.6 N/mm
$Spring3_Z$	892.4 N/mm
$Spring4_X$	11 755.6 N/mm
$Spring4_Y$	811.1 N/mm
$Spring4_Z$	935.5 N/mm

Table 10. Platform EMA vs FEA updated modal properties

Mode	**Description**	**EMA Freq(Hz)**	**FEA Freq(Hz)**	**% Diff)**	**MAC**
1	side-side	5.82	5.76	-0.89	0.909
2	bounce	7.28	7.60	4.31	0.900
3	rock side-side	9.78	8.81	-9.86	0.975
4	rock fore-aft	12.71	13.10	3.01	0.733
5	twist	15.69	15.75	0.398	0.693
6	first torsion	22.92	28.99	26.5	0.963
4	first bending	28.85	32.09	11.25	0.676

which were described above. The flexible dynamics of the tower and base structure are much higher in frequency range than the operating range of the turbine, so standard material models and measurements were used for these parts. Point masses of 200 g were added to simulate the effect of the mounting hardware for the blades and struts. Mass-less rigid connections were made between adjacent nodes to tie the model together. There was no additional model tuning in the fully assembled system.

The correlation of a subset of modes of the full turbine system is given in Table 11. Overall the model is able to capture the turbine dynamics well. The first rigid body modes of the system match well in frequency and shape especially the side-side and vertical bounce modes. The turbine based flexible modes are also represented well matching frequency to within 0.6% and accurately in mode shape with a MAC value of up to 0.918. The fact that these modes match so well is evidence that the assumptions used in the connecting of the independent models are valid. Figure 19 shows the EMA and FEA mode shapes side by side.

6. Conclusion

A set of characterization tests were performed on the PitchVAWT turbine and components. These data were used to update finite element models of the turbine at multiple levels of fidelity. Results of the individual component tests were as to be expected from initial finite element modeling. The specific cross sectional areas and material quantities required only slight adjustments from the expected values in the as-built condition. However, in the full system configuration the dynamics of the platform structure play a significant role in the turbine

Table 11. Full turbine EMA vs FEA

Mode-pair	EMA Freq(Hz)	FEA Freq(Hz)	% Diff)	MAC
1	5.50	5.64	2.54	0.869
2	6.41	6.44	0.51	0.820
3	7.06	6.65	-5.74	0.844
4	7.71	8.11	5.15	0.839
5	11.29	12.99	15.03	0.611
6	12.96	14.45	11.44	0.658
7	19.65	19.68	0.16	0.859
8	20.77	20.63	-0.65	0.918
9	26.16	28.93	10.58	0.806

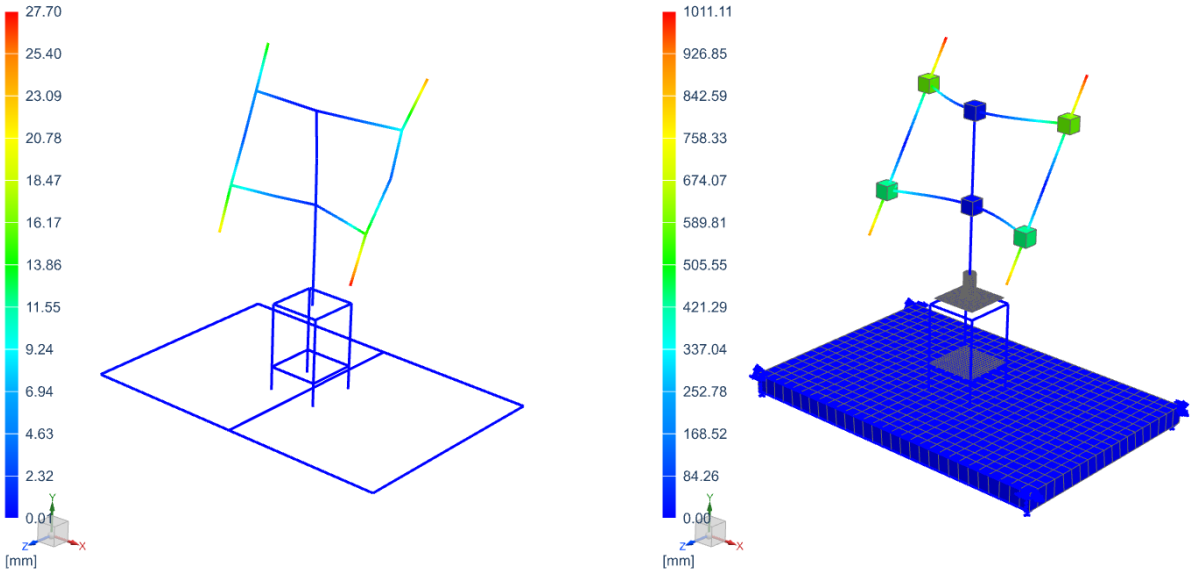

Figure 19. Rotor rocking in phase left: EMA 20.77 Hz right: FEA 20.56 Hz MAC: 0.89

response at specific frequencies of interest. Therefore the model has been updated to reflect these results and the table dynamics are considered in the turbine response. Several insights were gained into the structural behavior of the system including the large effects of the flexible platform structure on the mode shapes and frequencies of the overall turbine. The updated finite element models are able to properly capture all dynamics of interest and will be used to predict turbine response due to dynamic pitching and base excitation during operational measurements in the Open Jet Facility wind tunnel at the Delft University of Technology.

References

[1] Huijs F, Vlasveld E, Gormand M, Savenije F, Caboni M, LeBlanc B P, Ferreira C S, Lindenburg K, Gueydon S, Otto W and Paillard B 2018 Integrated design of a semi-submersible floating vertical axis wind turbine (vawt) with active blade pitch control
[2] Ennis B L, White J R and Paquette J A 2018 Wind turbine blade load characterization under yaw offset at the swift facility
[3] Vlasveld E, Huijs F, Savenije F and Paillard B 2018 Coupled dynamics of a vertical axis wind turbine (vawt) with active blade pitch control on a semi-submersible floater
[4] LeBlanc B P and Ferreira C S 2018 Overview and design of pitchvawt: Vertical axis wind turbine with active variable pitch for experimental and numerical comparison

[5] LeBlanc B P and Ferreira C S 2018 Experimental determination of thrust loading of a 2-bladed vertical axis wind turbine
[6] Veers P S, Laird D L, Carne T G and Sagartz M J 1998 Estimation of uncertain material parameters using modal data
[7] Griffith D T, Paquette J A and Carne T G 2008 Development of validated blade structural models
[8] Griffith D T and Carne T G 2010 Experimental modal analysis of 9-meter research-sized wind turbine blades
[9] Carne T G and Nord A R 1982 Modal testing of a rotating wind turbine Report Sandia National Laboratories
[10] James G H I, Carne T G and Lauffer J 1995 *The International Journal of Analytical and Experimental Modal Analysis* **10** 17
[11] Manzato S, White J R, LeBlanc B P and Peeters B 2013 Development of techniques for enhanced operational modal analysis of wind turbine
[12] LeBlanc B P, Cloutier D and Marinone T 2014 Overview of the dynamic characterization at the doe/snl swift wind facility
[13] Allemang R J and Brown D 1982 A correlation coefficient for modal vector analysis
[14] Allemang R 2003 *Sound and Vibration* 8